Kinetics of Secondary Carbides Precipitation in a High-Chromium White Iron

A. Bedolla-Jacuinde, L. Arias, and B. Hernández

(Submitted 26 March 2003)

This work analyzes the rate of secondary carbides precipitation during the destabilization heat treatment of a 17%Cr white iron. The experimental iron was characterized in the as-cast conditions to have comparable parameters with the heat treated samples. Destabilization heat treatments were undertaken at temperatures of 900, 1000, and 1150 °C for between 5 min and 8 h; each sample was water quenched immediately after being taken out of the furnace. Characterization was carried out by optical and electron microscopy, image analysis, and energy dispersive spectroscopy (EDS) microanalysis; hardness and microhardness were also evaluated. It was found that most of the secondary carbides that precipitate (between 2-30% of the matrix volume) precipitated in less than 2 h for the lowest destabilization temperature (900 °C). The secondary carbides volume fraction was found to increase for lower destabilization temperatures and large soaking times. A very low carbide precipitation along with a stabilization of the austenite phase occurred for heat treatments at 1150 °C. The results are discussed in terms of the solubility of chromium and carbon in the austenite phase at the different treatment temperatures.

Keywords cast iron, high-chromium, secondary carbides

1. Introduction

High-chromium white irons are ferrous alloys containing between 11-30%Cr and 1.8-3.6%C. It is also common to find some alloying elements such as molybdenum, manganese, copper, and nickel. The typical as-cast microstructure of these alloys consists of primary and/or eutectic carbides (M_7C_3) in a metastable austenitic matrix.[1] The hard eutectic carbides are mainly responsible for the good abrasion resistance of these alloys. Therefore, these alloys have been widely used for applications where stability in severe environments is the main requirement, such as the mineral processing industry, cement and paper production, and the steel manufacturing industry.[2] Both carbides and matrix contribute to wear resistance and fracture toughness. Eutectic carbides have a hexagonal crystalline structure and solidify as colonies of plates or bars (eutectic grains). Once solidified, carbide morphology is relatively immune to a subsequent modification by heat treatment. The as-cast austenitic structure, in contrast, is readily heat treated for destabilization and for obtaining small secondary carbides precipitated in a matrix that is a mixture of martensite and retained austenite.[3]

The commonly applied heat treatment for maximum strengthening is denoted destabilization, which consists of heating the alloy at temperatures within 800-1100 °C, soaking at these temperatures, followed by an air quenching at room temperature. During soaking, carbon and chromium from the matrix react to form small-distributed carbide particles. The new chromium- and particularly carbon-depleted matrix readily transforms to martensite during the subsequent cooling down. Therefore, the final structure after destabilization consists of M_7C_3 eutectic carbides and a martensitic matrix with secondary carbides distributed in it.[1] Secondary carbide precipitation and the transformed martensitic matrix promote an even more brittle alloy. However, a martensitic matrix is recommended to obtain greater hardness and better wear properties; but this increase in hardness affects fracture toughness. Such a phenomenon brings attention to the importance of operation factors of the destabilization treatment to be studied to determine the appropriate temperature and soaking time for such a high level of hardness and fracture toughness.

Although relatively little systematic research on the secondary carbide precipitation phenomena and their effect on the iron matrix have been developed, some works regarding this field are relevant.[4-9]

2. Experimental Procedure

The experimental white iron for the present work was made in a vacuum induction furnace by using high purity raw materials, therefore obtaining an impurities-free well-controlled chemical composition alloy. The melt was poured at 1450 °C into a metallic mold placed within the vacuum chamber and a 6 cm diameter and 10 kg bar ingot was obtained. The ingot was sectioned with an alumina abrasive cutting wheel in a DISCOTOM (Buehler Inc., Waukegan, IL) by copious water amounts. The cutting process, manually controlled, was as slow as possible to avoid overheating the sample and rectangular 12 × 12 × 4 mm samples were obtained.

Destabilization heat treatments were undertaken in a furnace using electric heating elements at an air atmosphere. A complete series of 10 samples was placed into the furnace for a heat treatment; once the desired temperature was reached, the samples were periodically taken out and water quenched to ensure that the secondary carbides had precipitated during the

A. Bedolla-Jacuinde, L. Arias, and **B. Hernández,** Instituto de Investigaciones Metalúrgicas, Universidad Michoacana de San Nicolás de Hidalgo, Morelia, Michoacan, C.P. 58000, México. Contact e-mail: abedolla@zeus.umich.mx.

soaking time only. Heat treatments were undertaken at 900, 1000, and 1150 °C for a range of 5 min and 8 h.

Materials characterization in both as-cast and heat treated conditions was undertaken by optical and electronic microscopy, energy dispersive spectroscopy (EDS) microanalysis, x-ray diffraction (XRD), and image analysis.

Samples were prepared for metallography in the traditional way: grinding on abrasive paper of different mesh sizes (80, 180, 320, 400, 600, and 1200). Samples were then polished on nylon cloth with 6 μm diamond paste as the abrasive and then with 1 μm paste. Etching was carried out with two different solutions depending on the purpose: Villela's etchant (5 ml HCl and 1 g picric acid in 100 ml ethanol) for 30-60 s to reveal the microstructure, and a solution of 50 ml $FeCl_3$ plus 20 ml HCl in 930 ml ethanol, where the samples were immersed for about 3 h, for a deep etching. This latter etching readily removes part of the matrix on the surface allowing the naked carbides to be observed.

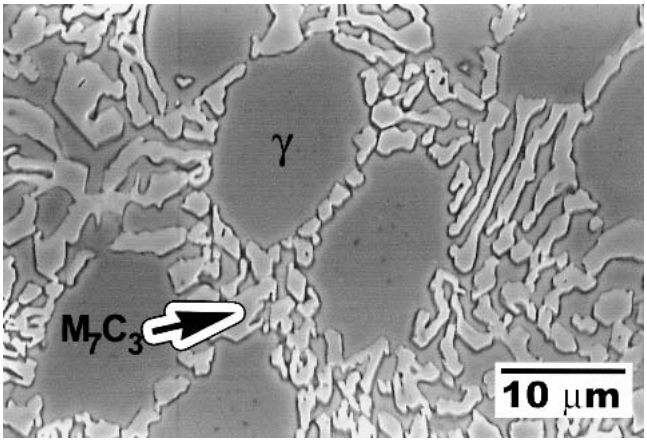

Fig. 1 Microstructure of the as-cast experimental iron showing pro-eutectic austenite areas (γ) and the austenite-M_7C_3 eutectic; scanning electron microscopy (SEM), Villela's etching 30 s

As-cast eutectic carbide volume fraction was measured by image analysis on digitized micrographs obtained at 250X on a Nikon EPHIPHOT 3000 inverted metallurgical microscope (Nikon, Melville, NY). For this purpose, the samples were deeply etched, and 20 micrographs were processed by the Sigmascan (Jandel Scientific, San Rafael, CA) V.5 software on a PC.

XRD studies were also undertaken to identify the different phases present in the alloy both before and after heat treatment. Retained austenite quantification was also calculated by XRD data by the technique described by Kim.[10] XRD tests were carried out by using Cu-Kα radiation in a 2θ range of 30-130°. Further characterization was undertaken on a JEOL (JEOL, Peabody, MA) 6400 SEM at 20 kV for imaging and microanalysis, and a PHILIPS TECNAI TEM (Philips, Eindhoven, The Netherlands). Secondary carbides volume fraction and size was obtained by point counting measurements on SEM micrographs by using a transparent 250 point grid.

Bulk hardness and microhardness of the matrix were undertaken on metallographic samples. Twenty tests for each sample were carried out by a diamond indenter and a 50 g load for 15 s, for Vickers microhardness (HV_{50}). Bulk hardness was undertaken in the Rockwell C scale.

3. Results and Discussion

Table 1 shows the chemical composition of the experimental high-chromium white iron, 16.9%Cr and 2.58%C, one of

Table 1 Chemical Composition of the Experimental White Iron, wt.%

Carbon	Chromium	Molybdenum	Nickel	Vanadium	Sulphur	Phosphorus
2.58	16.90	1.98	1.80	1.98	0.007	0.006

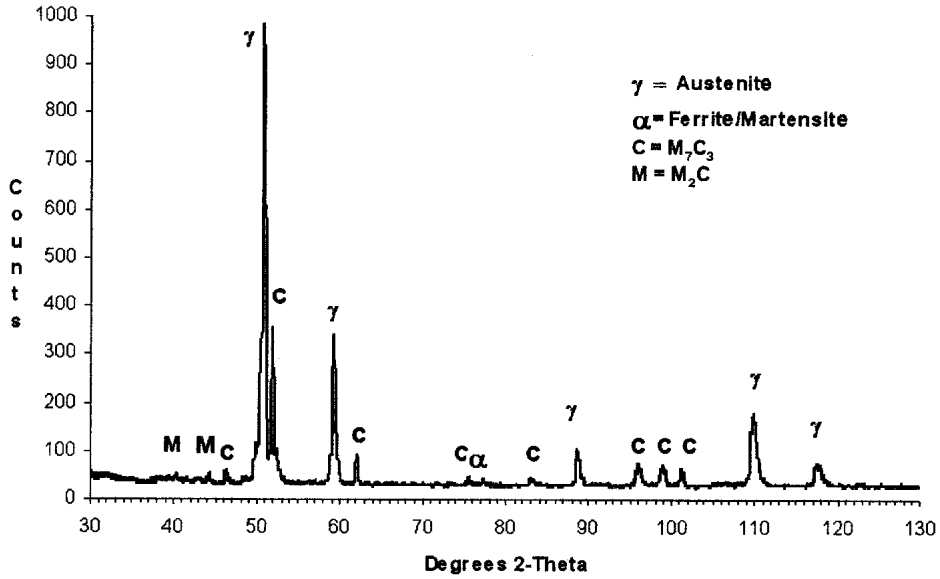

Fig. 2 XRD pattern of the as-cast alloy showing the presence of austenite γ, eutectic carbides M_7C_3, and carbides type M_2C

the most commercial high-chromium iron alloys.[1] Molybdenum and nickel contents are close to 2%, enough to ensure a good hardenability. Also, 2% vanadium was added to this iron for further hardness. Higher as-cast hardness values in these alloys have been reported when adding 2% vanadium as this element partitions almost totally to the eutectic carbide making the composition $(Fe,Cr,V,Mo)_7C_3$. Vanadium increases the hardness of the eutectic carbide and also the carbide volume fraction, which in turn increases the hardness of the alloy.[11]

3.1 As-Cast Structure

Figure 1 shows the typical as-cast structure of the alloy where the austenitic matrix and eutectic carbides can be observed. Because the alloy is hypoeutectic, austenite dendrites are the first to solidify followed by the eutectic. Only eutectic carbide and matrix phases can be observed from this picture; however, two additional phases are present as shown by XRD traces from Fig. 2. These additional phases present in small amounts are martensite and a molybdenum rich carbide type M_2C. Micrographs at higher magnifications show the presence of martensite at the matrix/carbide interface in the eutectic zones (Fig. 3). It has been widely reported that martensite forms due to the carbon and chromium depletion by diffusion towards the carbide during the solidification and the subsequent cooling to room temperature.[3,12,13] The martensite amount, as measured by XRD, is about 6%. The presence of the M_2C carbide was also detected by EDS in the SEM. Figure 4 shows the morphology and composition of this carbide; being a molybdenum rich carbide its composition is of the type M_2C, typical for molybdenum carbide. The main role of molybdenum in these irons is to improve hardenability; however, not all the molybdenum contributes to this goal. The presence of carbon leads to the formation of the molybdenum rich carbide and part of the molybdenum in these irons forms a eutectic carbide type M_2C at the end of the solidification stage.[14-19]

The elements distribution was analyzed by EDS in a random area of the as-cast microstructure. Figure 5(a) shows an SEM micrograph where some microanalyses were undertaken on the matrix (Fig. 5b), on the carbide (Fig. 5c), and on a scan along the line shown on the micrograph in Fig. 5(a), across an austenite dendrite arm (Fig. 5d).

Eutectic carbides are of the type M_7C_3 as revealed by XRD (Fig. 2) and as reported for chromium contents of 17%.[7] The elements present in the carbide phase can be seen from Fig. 5(b); despite being a qualitative analysis, the intensity of the peaks indicates that chromium and iron are present in higher amounts in the carbide. The carbide contains also vanadium and maybe small amounts of molybdenum, which could not be detected. However, the most important thing to highlight is the presence of vanadium in the eutectic carbide. XRD traces did not show the presence of vanadium carbide. Vanadium is a carbide-forming element of the type VC; however, the solidification temperature for this carbide is below the solidification temperature for the alloy. Therefore, vanadium carbide forma-

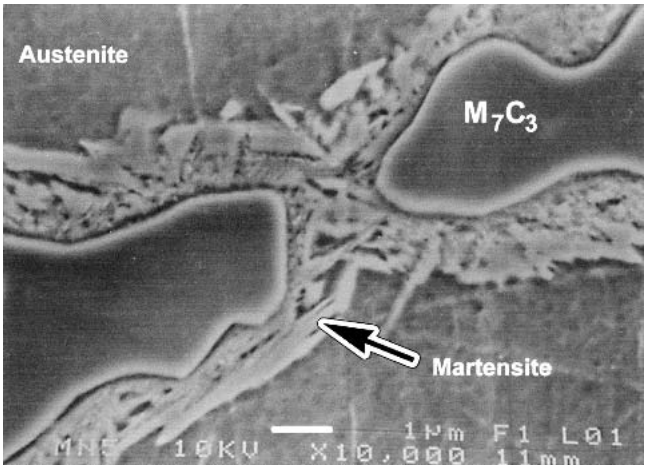

Fig. 3 SEM micrograph showing the presence of martensite at the matrix/carbide interface; Villela's etching, 45 s

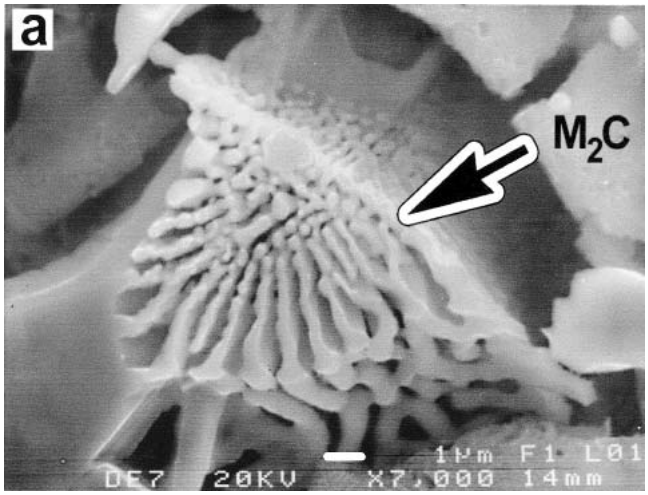

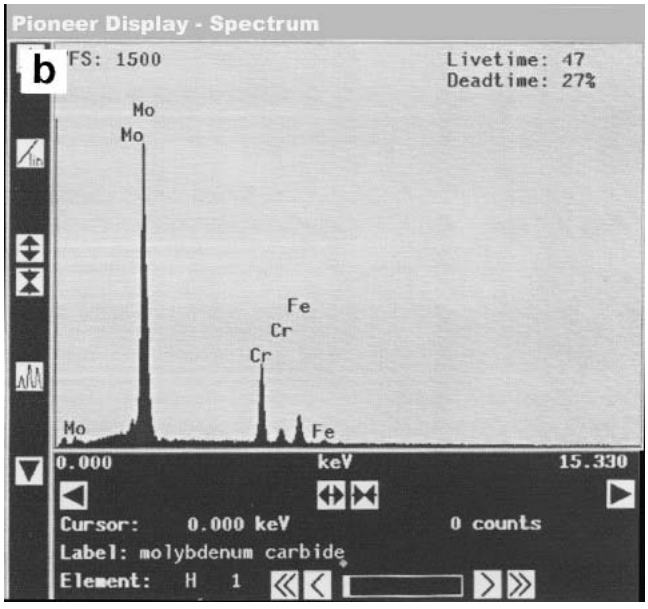

Fig. 4 **(a)** SEM micrograph of a deep-etched sample showing a molybdenum rich carbide type M_2C formed at the last solidification stage, etching solution 50 ml $FeCl_3$ plus 20 ml HCl in 930 ml ethanol for about 3 h; **(b)** EDS of the M_2C carbide in (a)

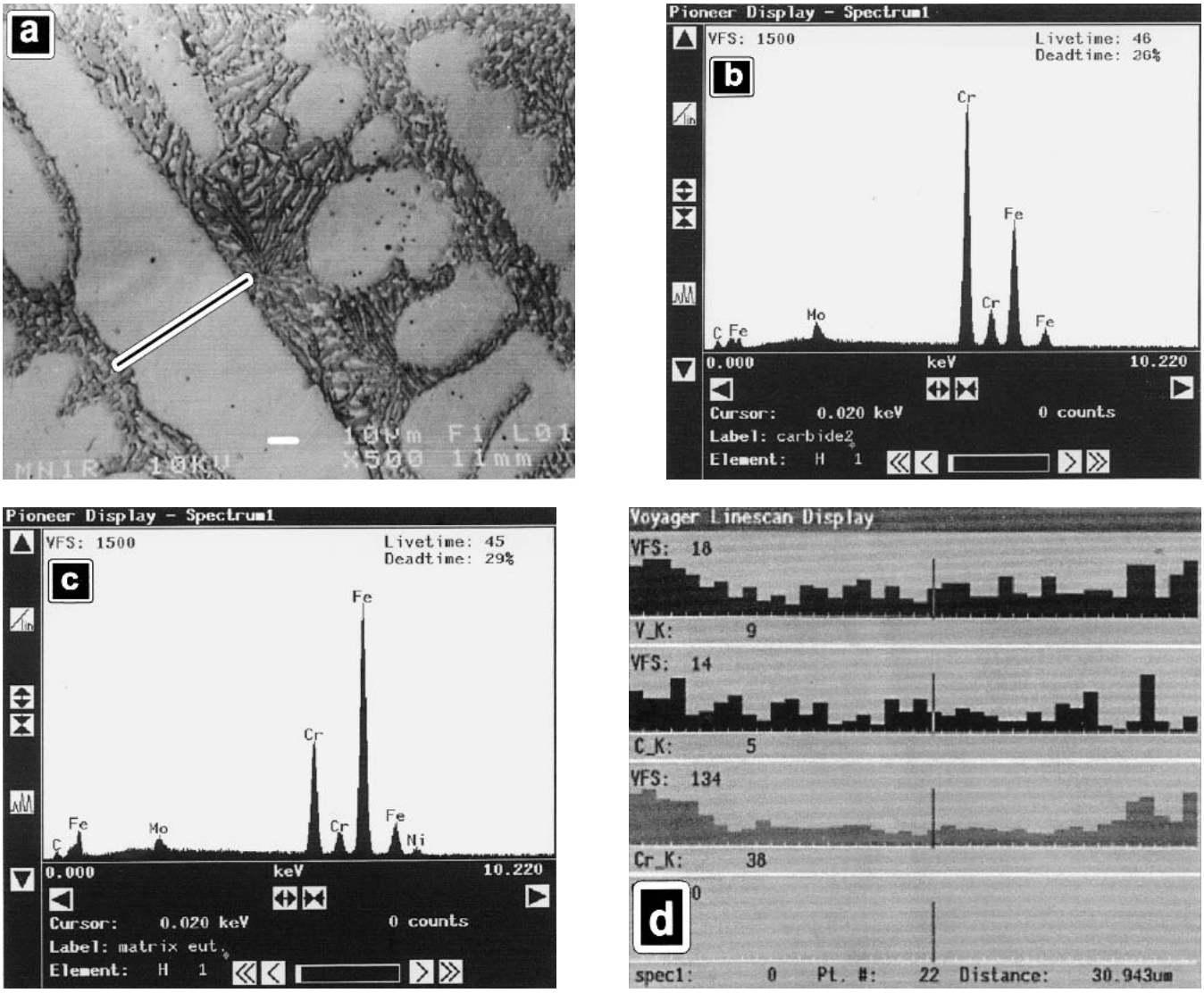

Fig. 5 **(a)** SEM micrograph of the structure of the as-cast experimental iron, **(b)** EDS corresponding to the eutectic carbide phase, **(c)** EDS corresponding to the proeutectic matrix, and **(d)** vanadium, chromium, and carbon profile of matrix along the line shown in (a)

tion in this kind of irons is not likely. These vanadium carbides are believed to form only when the vanadium content exceeds 3% as reported by Radulovic et al.[20] Therefore, the major proportion of vanadium partitions to the carbide and the rest remains dissolved in matrix, as shown in the EDS in Fig. 5(c). A minor proportion of chromium related to iron can be observed from this spectrum, contrary to the findings in the carbide microanalysis where the chromium:iron ratio is close to 1. A high amount of molybdenum is also observed in matrix. This element remains in matrix in major proportion contributing this way to improve hardenability. From the same spectrum in Fig. 5(c), to the right of the last iron peak, a small peak corresponding to nickel can be observed. Nickel remains totally in matrix, contributing synergistically with molybdenum to hardenability. Vanadium can also be observed in matrix but in much smaller amounts than in the eutectic carbide. The scan on the line in Fig. 5(a) shows the presence of chromium, carbon, and vanadium in matrix; a higher proportion of these elements is observed at the edges of the graph. These ends include the carbide phase as seen from the line. The presence of these elements in matrix is the source for secondary carbides precipitation during the heat treatment of austenite destabilization.

Eutectic carbide is a very important phase in the properties of these alloys. It has been mentioned that eutectic carbide is a 3D network or an interconnected skeleton into the material; however, the level of interconnection is much less than in unalloyed white irons. This is due to the differences in preferential growing directions for cementita and the carbide M_7C_3. M_7C_3 carbide has a hexagonal structure and a preferential growing direction <0001> [7]; therefore, the typical morphology of these carbides is bars or plates (Fig. 6). On a polished surface these bars could be perpendicular to the surface, appearing to be isolated particles under the microscope; however, deep-etching techniques on the SEM make it possible to observe that many bars may be separated at the surface but connected at the base.

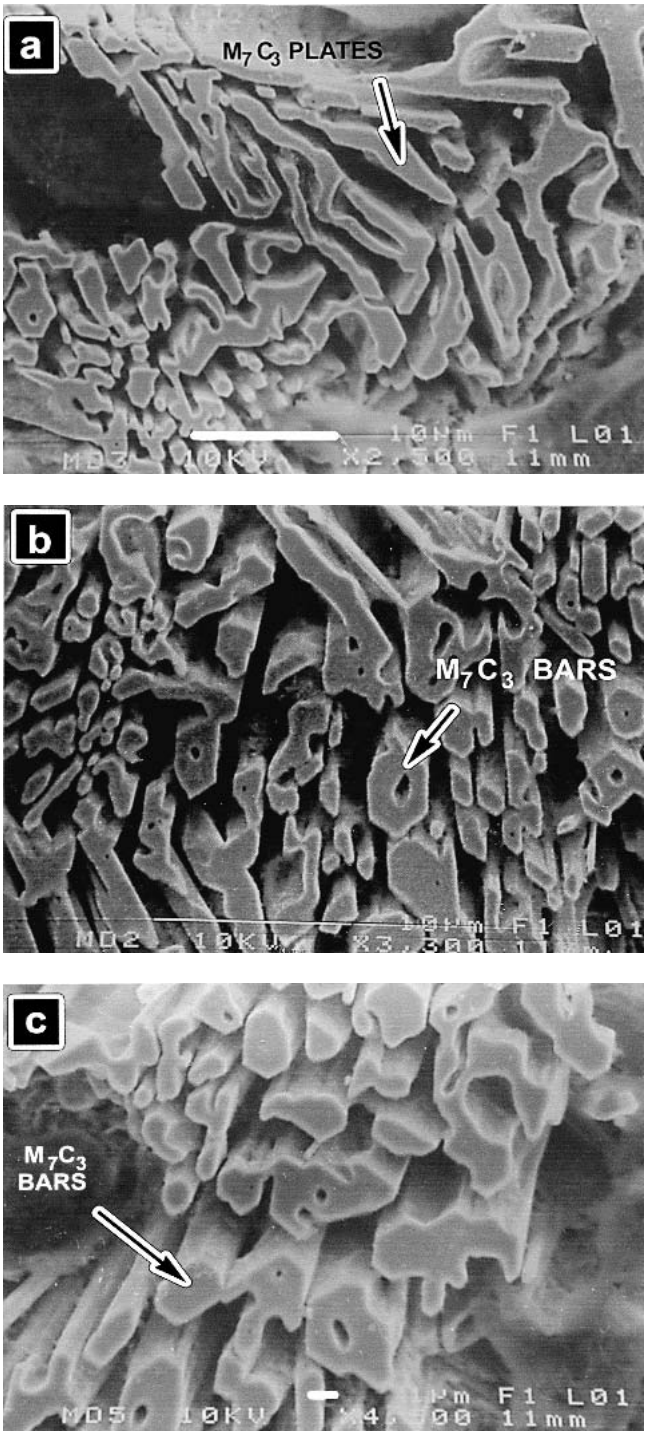

Fig. 6 SEM micrographs with the 3-D structure of eutectic carbides showing the real morphology; deep-etching with a solution of 50 ml $FeCl_3$ plus 20 ml HCl in 930 ml ethanol for 3 h

3.2 Structure After Destabilization Heat Treatment

After destabilization heat treatment, some phenomena took place, which altered the structure of the material. Such phenomena are a function of temperature and soaking time as in any heat treatment. The phases present in the as-cast alloy are the same as in the heat treated samples, but the proportion has changed. The XRD pattern from Fig. 7 is a representative proof of what happens after heat treatment. The present phases are austenite, martensite, M_7C_3 carbide, and M_2C carbide. The main difference that can be observed from this XRD compared with that from Fig. 2 (as-cast material) is the higher intensity for the martensite peaks (α phase). Therefore, the amount of martensite is higher in the heat treated samples, except in those treated at 1150 °C where the austenite phase was overstabilized (see Section 3.5). According to the XRD traces, secondary carbides precipitated in matrix are of the type M_7C_3, the same as the eutectic, because no other type was detected. The kind of secondary carbides precipitating depend on the alloy composition and the destabilization temperature. The presence of secondary carbides of the type $M_{23}C_6$ has been observed as fine interconnected bars in irons with very high chromium amounts (>25%).[5,7] On the other hand, secondary carbides of the type M_7C_3 were observed as agglomerated plates in irons with chromium contents between 15-20%.[5] These results agree with the findings in the present work.

3.3 Secondary Carbide Volume Fraction

Figure 8 shows the obtained results for the volume fraction of secondary carbides precipitated as a function of the soaking time for each of the studied temperatures; the horizontal axis, which corresponds to time, is plotted in logarithmic scale. At 900 °C, precipitation was observed to start at about 10 min and a volume fraction of 2% was measured; after 8 h of treatment the volume fraction was about 27%. At 1000 °C the precipitation process was faster, 2% at 5 min up to 21% at 10 min; from 10 min to 8 h, the volume fraction was about 22%. The total volume fraction precipitated within the first 10 min; afterwards the coarsening of some carbides and the dissolution of others occurred.

At 1150 °C a volume fraction of 15% occurred at only 5 min; subsequently the volume fraction diminished to 2% at 1 h soaking. Figures 9, 10, and 11 show sequences of SEM micrographs of some samples at different soaking times and at the temperatures of 900, 1000, and 1150 °C, respectively. These series of micrographs represent visually what is plotted in Fig. 8. At 900 °C the diffusion rate of chromium and carbon lead to volume fraction of secondary carbides of 27% in 8 h. However, most of the precipitation took place within the first 2 h, which is not clear because the scale of time is plotted logarithmically. Higher temperatures, such as 1000 °C, accelerated the precipitation process due to the higher diffusion rate of the elements that form the carbides, chromium, and carbon. At this temperature almost all of the volume of secondary carbides precipitated within the first 10 min, reaching a total volume fraction of 22%. In contrast, at 1150 °C where diffusion rates for chromium and carbon are higher, a carbide precipitation of 15% was observed within the first 5 min, but it started to diminish afterwards. It is likely that the initial amount of carbides had precipitated during heating to the soaking temperature and these carbides dissolved during soaking when the equilibrium composition of chromium and carbon in austenite was reached. According to the Fe-C phase diagram, austenite can dissolve higher carbon contents as the temperature increases to the eutectic.

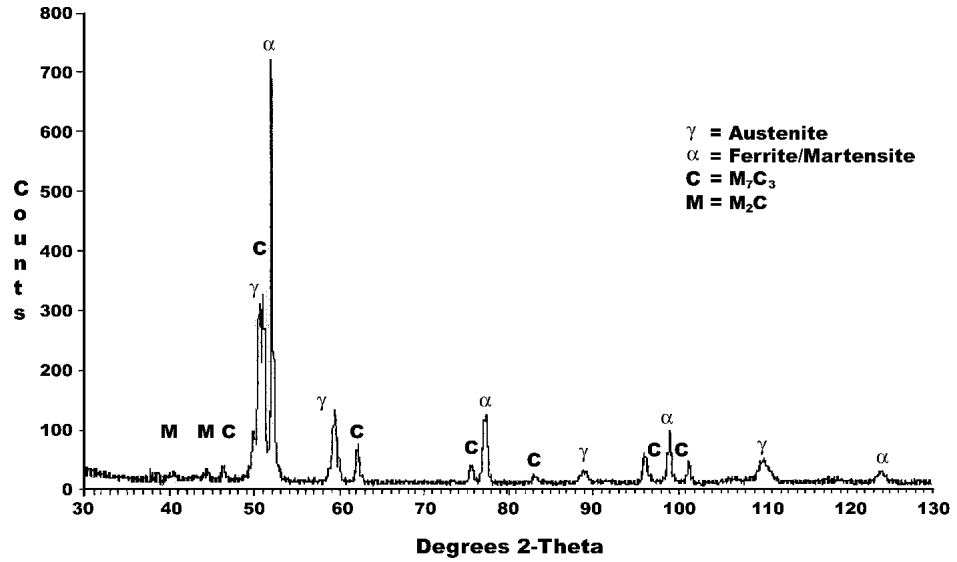

Fig. 7 XRD pattern of the simple destabilized at 1000 °C for 1 h showing the detected phases, austenite, martensite, M_2C, and M_7C_3

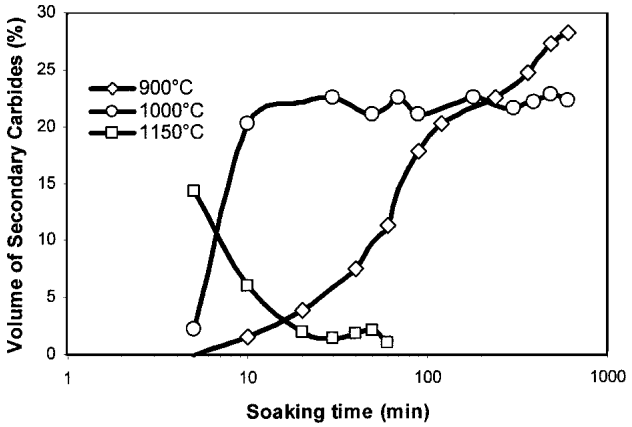

Fig. 8 Volume of secondary carbides precipitated as a function of the soaking time during destabilization for each of the studied temperatures

As mentioned, at 900 °C a higher secondary carbide volume fraction was observed; at lower temperatures, the ability of austenite to dissolve carbon is lower. Therefore, there is a higher amount of carbon to precipitate, which in turn is observed as a higher carbide volume fraction. At higher temperatures, austenite can retain carbon and chromium in higher amounts, so there is very low raw material available to precipitate carbides,[5,8,9] and the final volume fraction is much lower. It is difficult to explain the diminishing of carbide volume fraction observed at 1150 °C; it is likely the equilibrium concentration of carbon in austenite will be higher than the actual amount of this element in austenite, so that, during soaking precipitation is void. Perhaps the volume fraction in the first sample (15% at 2 min) precipitated during heating to the soaking temperature and these 2 min at 1150 °C were not enough for austenite to reach its equilibrium composition and the secondary carbides did not dissolve. Samples treated for longer times (10 and 60 min) show a precipitated volume fraction of 2-5%; perhaps the equilibrium volume in the alloy is at 1150 °C.

From micrographs in Fig. 9, 10, and 11, and particularly from Fig. 12, the morphology of secondary carbides can be observed. Secondary carbides are bars connected within the bulk matrix. It has been reported[5] in white irons of similar composition that secondary carbides precipitated after destabilization treatments are of the type M_7C_3, having a hexagonal structure and a preferred growing direction <0001>. Figure 13 shows some TEM micrographs of secondary carbides and a diffraction pattern of these particles, which agree well with the findings in Ref. 5.

3.4 Precipitated Carbides, Size, and Number

Figure 14 shows the particle size as a function of the soaking time; these measurements are taken as the diameter of the carbide bar. It is well known that precipitation processes are favored by temperature, because temperature accelerates diffusion of the elements dissolved in matrix. A higher diffusion rate of elements is observed for precipitation processes undertaken at high temperatures. Because precipitation takes place by nucleation and growth phenomena, particles of a certain size are formed, which depend on the treatment temperature. In the current study, when the iron was treated at 900 °C the secondary carbides diameter was about 120 nm within the first 2 h; afterwards, they coarsened up to 300 nm for 8 h soaking time. At temperatures of 1000 °C the initial diameter is close to 200 nm and gradually coarsens up to 250 nm for 8 h soaking time. According to this sequence it would be expected that the diameter of secondary carbides formed at 1150 °C to be higher; however, their size is only about 160 nm. Because the volume of material that precipitates in equilibrium as secondary car-

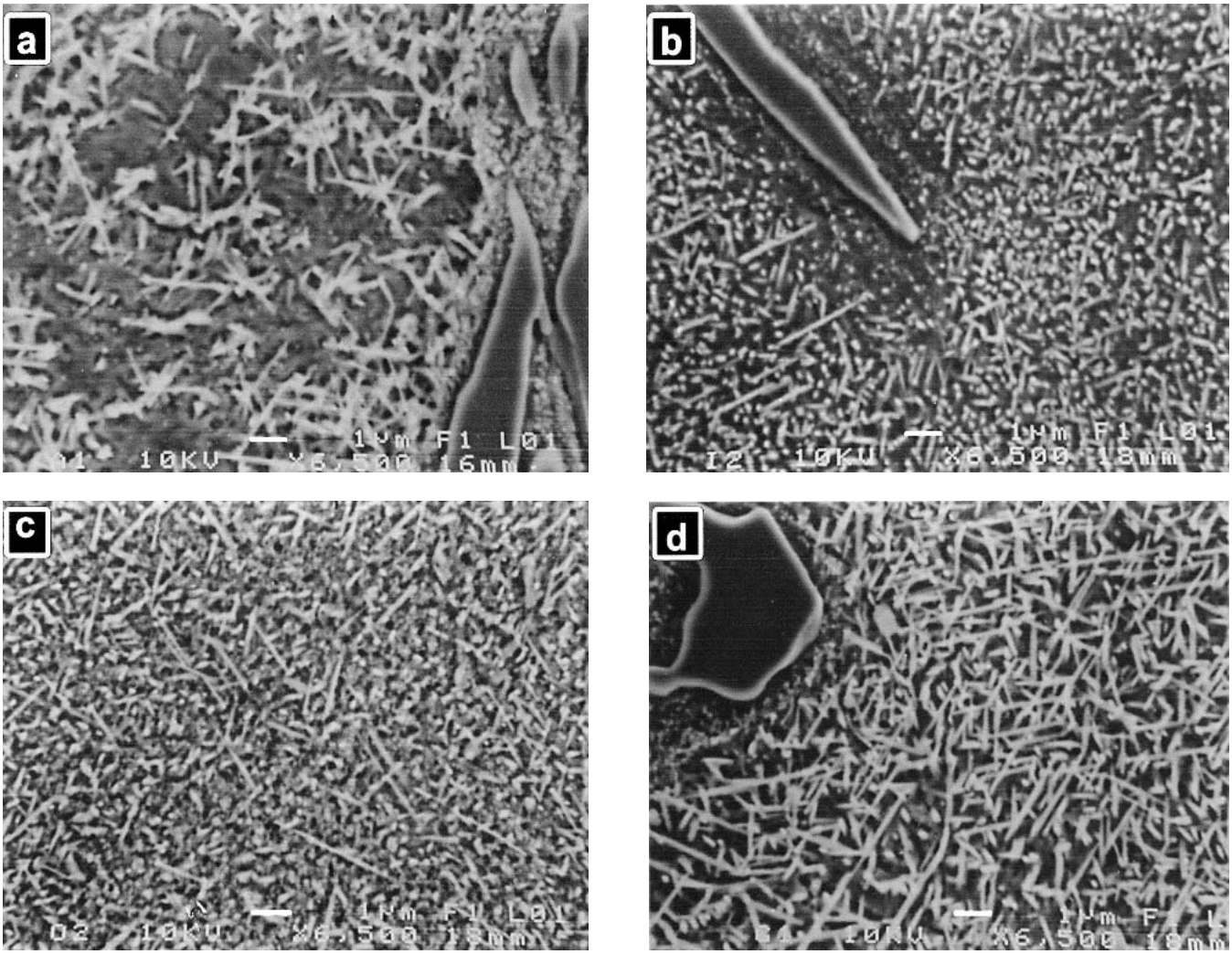

Fig. 9 Series of SEM micrographs showing secondary carbide precipitation during destabilization heat treatment at 900 °C of the experimental white iron. **(a)** 20 min, **(b)** 1 h, **(c)** 2 h, and **(d)** 8 h. Villela's etching, 45 s. Matrix is composed of martensite, retained austenite, and secondary carbides.

bides at this temperature is almost void, there is not enough material to precipitate coarse carbides.

What is important to highlight is the precipitation behavior at 900 and 1000 °C (Fig. 15). This figure shows the number precipitated particles per μm^2. At 900 °C the number of carbides went from 2 particles per μm^2 for 10 min soaking time to 14 particles for 90 min. Within the next 3 h the number of carbides remained at 14 and afterwards decreased to 8 particles per μm^2 for 8 h soaking time. This finding indicates that the precipitation process occurred during the first 90 min; during the next 3 h there was no new precipitation, just coarsening of the existing particles. Finally, during the next 4 h, dissolution of some carbides occurred contributing to the coarsening of some others thermodynamically more stable. Similar phenomena during destabilization heat treatments have been reported by Kuwano et al.[8] All these phenomena are better observed from SEM micrographs (Fig. 9, 10, and 11). Note that from the current study, the secondary carbides precipitation was observed homogeneously in matrix. According to Powell and Bee[9] and Bee et al.,[21] secondary carbides precipitate at slip bands and sub-grain boundaries within austenite. Such slip bands and sub-grain boundaries may form due to stresses generated by differences in the thermal expansion coefficients of carbides and matrix. On the contrary, Kuwano et al.[8] reported that the secondary carbides precipitation progressed from the periphery, adjacent to the eutectic carbides towards the center of the dendrite in low carbon irons. In high carbon alloys, the contrary occurred—precipitation progressed from the center of the dendrite towards the periphery. They attributed this phenomenon to chromium and carbon micro-segregation towards the periphery of the dendrites.

Just a few works on the kinetics of secondary carbide precipitation have been published. Powell and Laird[5] suggested that precipitation occurs during the first 25 min at the soaking temperature, and keeping the alloy for longer periods of time only causes coarsening of carbides. Kuwano et al.[8] felt that precipitation occurs within very short periods of time such as 1 min at temperatures between 950-1000 °C, which disagree with

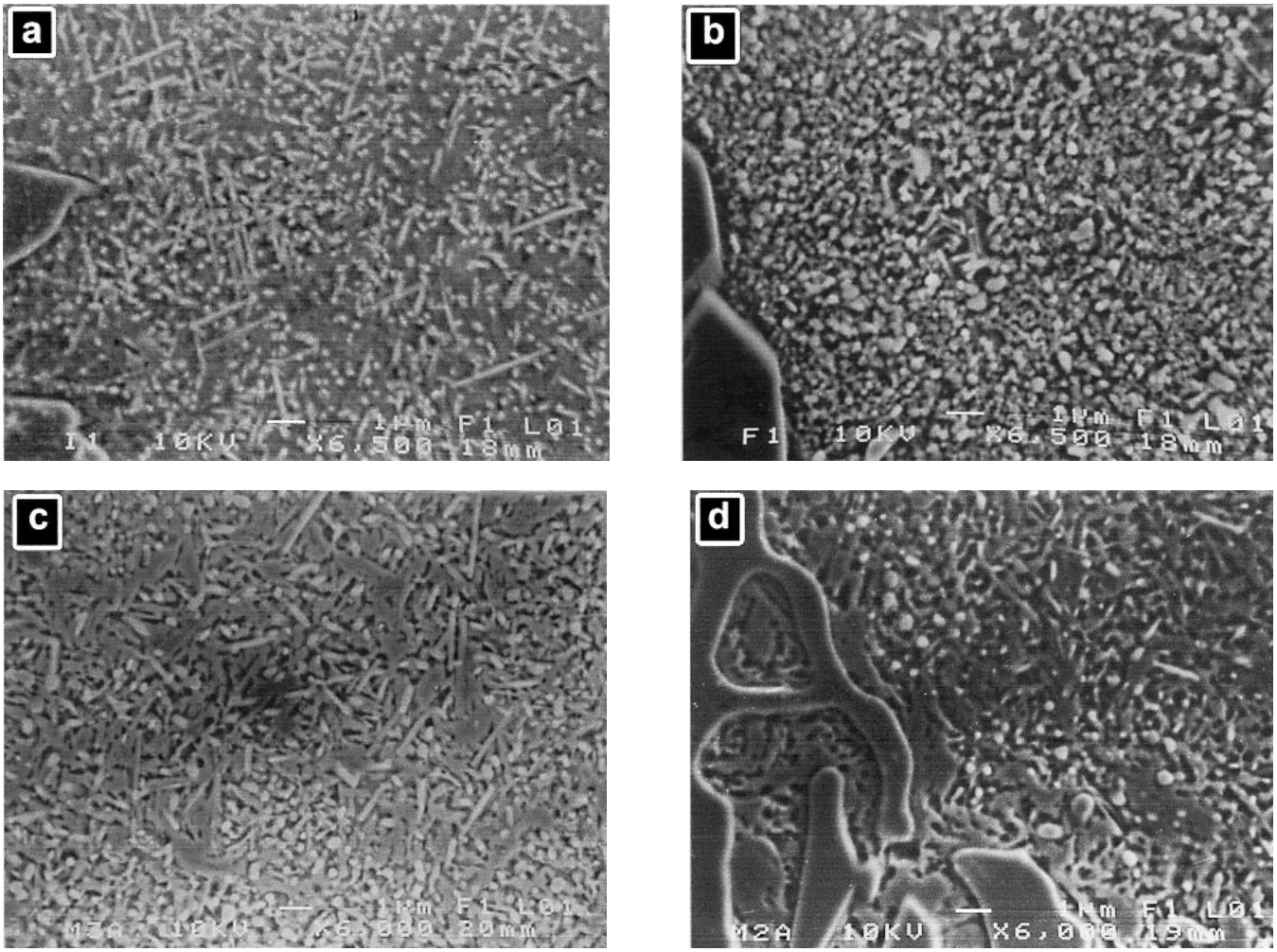

Fig. 10 Series of SEM micrographs showing secondary carbide precipitation during destabilization heat treatment at 1000 °C of the experimental white iron: **(a)** 5 min, **(b)** 10 min, **(c)** 1 h, and **(d)** 6 h. Villela's etching 45 s. Matrix is composed of martensite, retained austenite, and secondary carbides.

the findings from this work. What has been observed and widely accepted by most researchers is that once carbides have formed, longer periods of time at the treatment temperature increase the size and volume fraction of them. Furthermore, still longer periods of time at the soaking temperature cause the coarsening of carbides at the expense of others' dissolution (Ostwald ripening process), reducing the number of carbides.[8] This effect can be observed in Fig. 15.

3.5 Retained Austenite After Destabilization

Figure 16 shows the results of retained austenite as measured by XRD. As discussed above, secondary carbide precipitation depletes the austenitic matrix in chromium and carbon.[4,10] Such depletion produces an increase in M_S and it is more likely to obtain martensitic structures. Such an effect is observed in Fig. 16; at 900 °C and long soaking times, a reduction in the retained austenite content is observed from 48% at 10 min to just 8% for 8 h soaking time. This means an increase in the martensite volume fraction. At this temperature and long soaking times, the volume fraction of secondary carbides was 27%. The chromium- and carbon-depleted matrix transformed almost totally to martensite during the subsequent cooling. Something similar occurred during destabilization at 1000 °C; residual austenite decreased from 52% for 5 min soaking time to 15% for 8 h. In this case, the volume fraction of secondary carbides was less than in the alloy treated at 900 °C; a clear indication is that chromium and carbon dissolved in matrix are higher in the alloy treated at 1000 °C and such elements contribute to lower the M_S temperature. Therefore, the alloy treated at 1000 °C showed a higher amount of residual austenite. These results are in agreement with the findings of some authors[5,8,9] in high- and low-chromium white irons. On the contrary, retained austenite increased with soaking time for the iron treated at 1150 °C. For a 5 min soaking time, retained austenite was 25% and for 1 h the whole matrix became austenitic after heat treatment. In this case, the high temperatures allowed carbon and chromium to dissolve completely in matrix and inhibited the driving force for secondary carbides precipi-

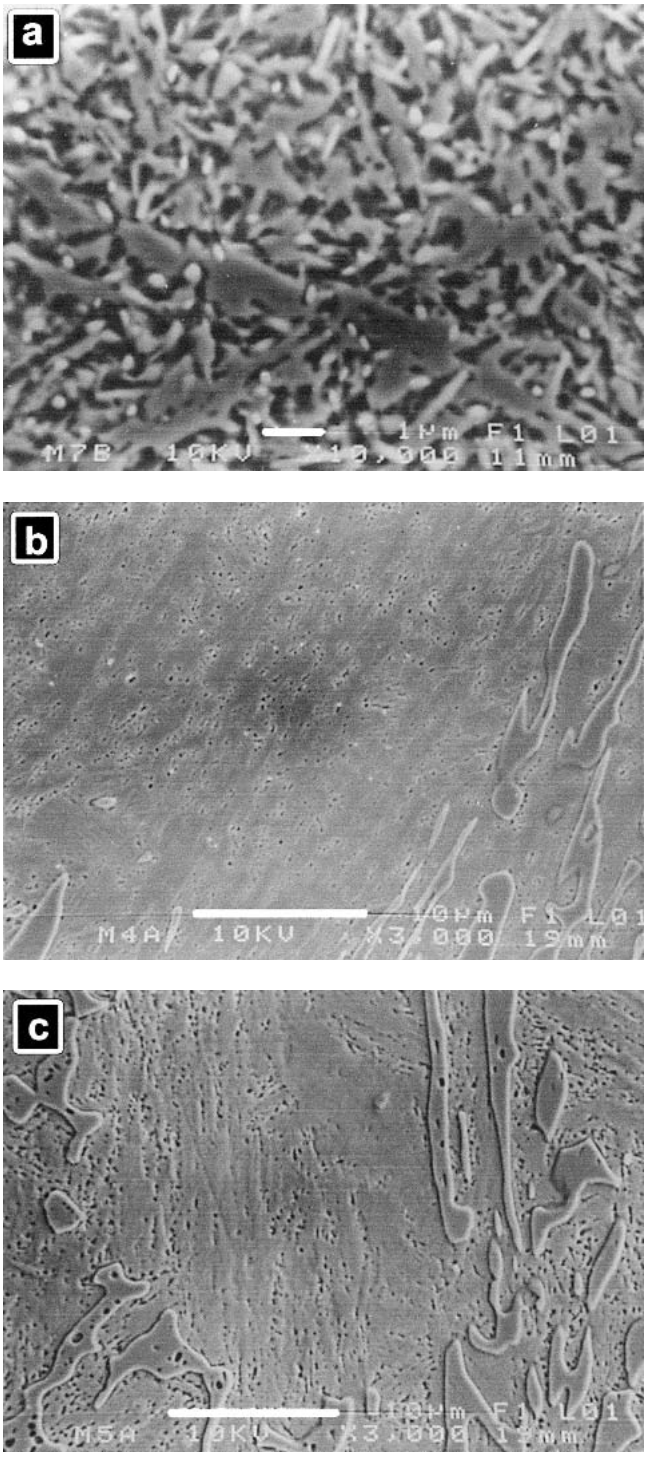

Fig. 11 Series of SEM micrographs showing secondary carbide precipitation during destabilization heat treatment at 1150 °C of the experimental white iron. **(a)** 2 min, matrix is composed of martensite, retained austenite, and secondary carbides; **(b)** 20 min, matrix composed of austenite mainly; and **(c)** 1 h, matrix is totally austenitic. Villela's etching 45 s

tation. Chromium- and carbon-rich austenite is stable under these conditions and remains stable during cooling to room temperature.[1,22,23]

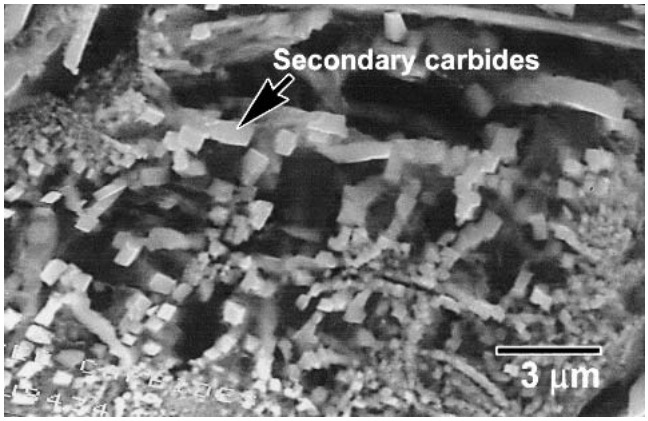

Fig. 12 SEM micrograph showing the real morphology of the secondary carbides precipitated during destabilization treatments. Deep-etching was with a solution of 50 ml $FeCl_3$ plus 20 ml HCl in 930 ml ethanol for 15 min.

3.6 Microhardness of Matrix and Bulk Hardness of the Alloy After Destabilization

Figure 17 shows the microhardness values obtained for the iron's matrix after each heat treatment. At 900 °C for 10 min, microhardness was $800HV_{50}$ and increased to a maximum of $1300HV_{50}$ after 2-3 h soaking time; afterwards it decreased to $900HV_{50}$ for a destabilization of 8 h. The increase in microhardness of the matrix is influenced by two factors as the soaking time increased: the precipitation of secondary carbides that strengthens the matrix by particle dispersion together with the increase in martensite volume fraction. However, diminishing microhardness after 3 h soaking time is attributed to the secondary carbide coarsening. At this stage, longer times promote a major diffusion of elements, favoring coarsening of some carbides at the expense of others' dissolution; such a phenomenon leads to a diminishing number of particles in the matrix (Fig. 15). The final structure of the matrix is therefore highly martensitic with relatively few coarse secondary carbides. For the structures of the irons with maximum hardness, a highly martensitic matrix was also observed but it contained a higher number of fine well-dispersed secondary carbides.

A similar effect occurred for the iron treated at 1000 °C; however, maximum hardness ($1159HV_{50}$) was obtained at shorter times (30-60 min). Higher destabilization temperatures allowed higher diffusion, leading to a reduced amount of coarse nuclei (Fig. 14 and 15). Under this situation, the strengthening due to dispersed particles is lower. Furthermore, at these higher temperatures, austenite can dissolve higher carbon contents, so that the amount of secondary carbides is also minor. The above phenomena lead to a higher retained austenite content in the final structure, which reduced matrix hardness.

In contrast, for the iron treated at 1150 °C, hardness of the matrix diminished since the beginning. For this case, a stabilized austenitic matrix was obtained. Such a matrix was solid solution strengthened by chromium, carbon, nickel, molybdenum, etc., but not by particle dispersion. Secondary precipitation occurred only in the early stages of the heat treatment.

Regarding bulk hardness, the alloy showed a behavior simi-

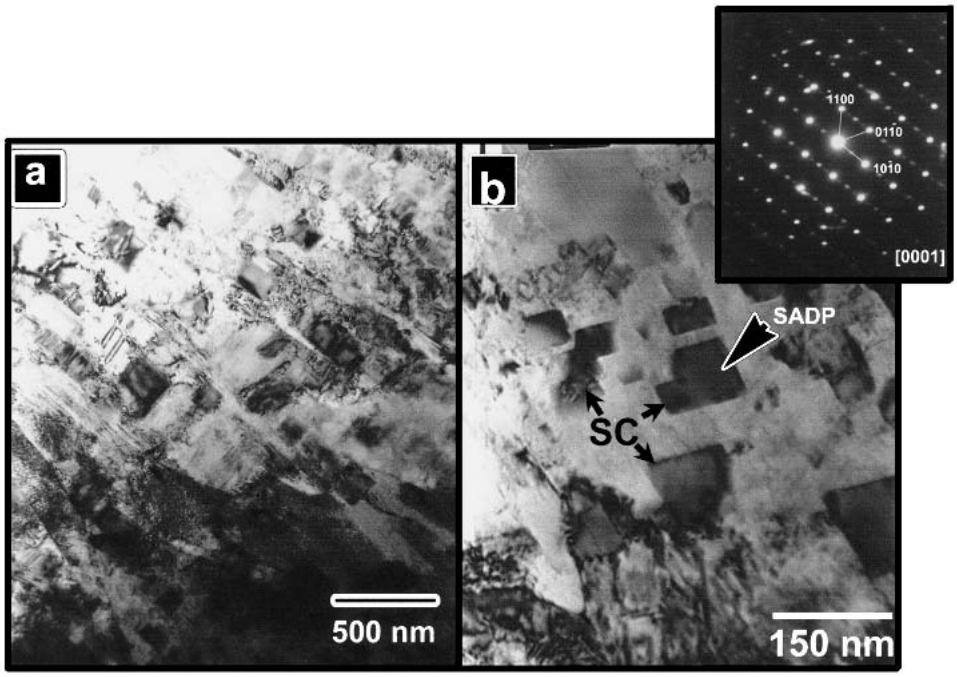

Fig. 13 Bright field TEM micrographs showing some secondary carbides (SC) in **(a)** sample treated at 900 °C for 1 h, and **(b)** sample treated at 1000 °C for 1 h. The selected area diffraction pattern (SADP) on the particle arrowed in (b) indicates the crystallographic nature of these carbides to be hexagonal M_7C_3.

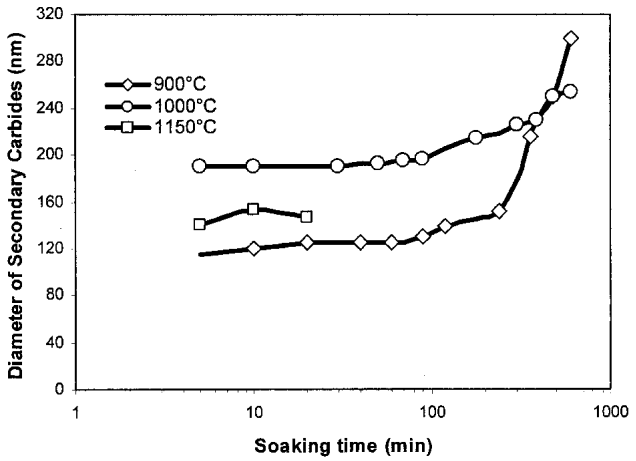

Fig. 14 Diameter of the precipitated particles as a function of the soaking time during destabilization heat treatment

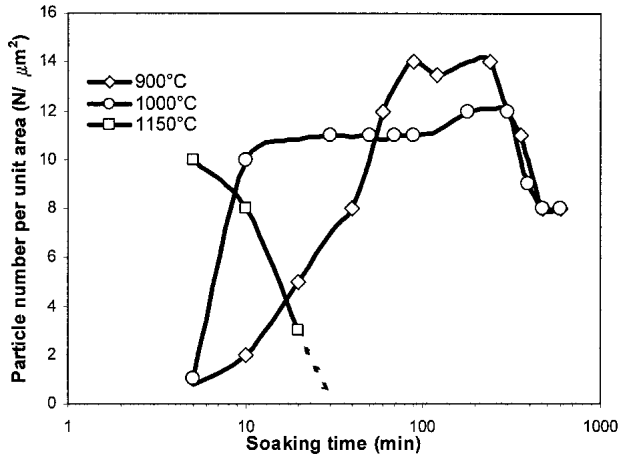

Fig. 15 Number of precipitated particles in a square micron (μm^2) as a function of the soaking time during destabilization heat treatment

lar to that for matrix microhardness. Figure 18 shows the results for hardness where maximum values can be observed for the different temperatures. For the iron treated at 900 °C, maximum hardness was 68 HRC and was obtained for1-2 h soaking time. For the iron treated at 1000 °C, maximum hardness was 60 HRC obtained for 30 min. Finally, for the iron treated at 1150 °C, hardness remains constant (45 HRC) during the first 20 min of treatment and decreases afterwards. The strengthening of the matrix is the main factor responsible for the modifications in the iron's hardness. Microhardness of matrix and the eutectic carbide volume fraction are the factors that contribute to strengthening of the alloys. For this case, the carbide volume fraction was constant (24%); therefore the strengthening of matrix caused the changes in bulk hardness.

These strengthening phenomena are similar to those found in aging processes of some alloys and are explained in terms of the diffusion of elements that participate in the precipitating phase. Such diffusion in turn is a function of treatment temperature and soaking time. Kuwano et al.,[8] Powell and Laird,[5] and Powell and Bee[9] have found similar behaviors for high- and low-chromium irons in studies of precipitation and hardness.

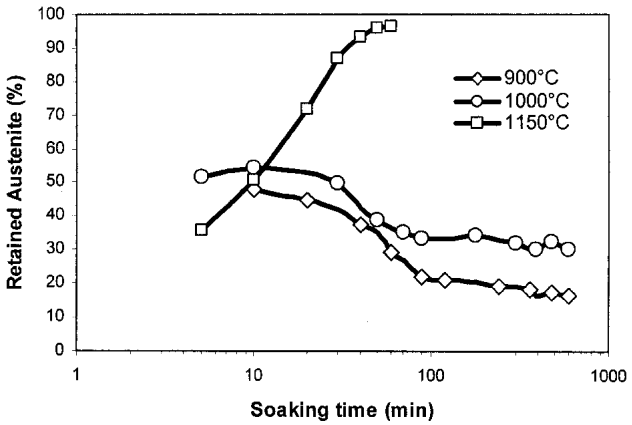

Fig. 16 Retained austenite content in iron matrix as a function of the soaking time during the destabilization heat treatment

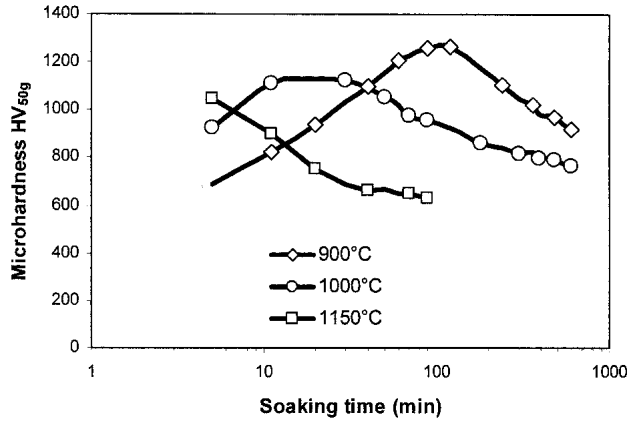

Fig. 17 Matrix microhardness as a function of the soaking time during the destabilization heat treatment

4. Conclusions

- The structure of the as-cast alloy was composed of 24% eutectic carbides, about 5% martensite, and 70% austenite; small amounts of the molybdenum-rich carbide Mo_2C were also present.
- Vanadium carbide was not detected in the alloy; nonetheless, the iron contained 2% vanadium, a carbide-promoting element. Vanadium was observed to partition to the carbide and in minor amounts to the matrix.
- According to the studied temperatures, the secondary carbide precipitation level decreased with higher temperatures, being the highest for the samples treated at 900 °C (27% of matrix).
- High temperatures like 1150 °C over-stabilized the austenitic matrix, which led to a secondary carbides free austenitic matrix after heat treatment.
- The amount of precipitated particles showed an increase with time for the samples treated at 900 and 1000 °C, reaching a maximum and then decreased due to dissolution of some carbides and coarsening of some others.

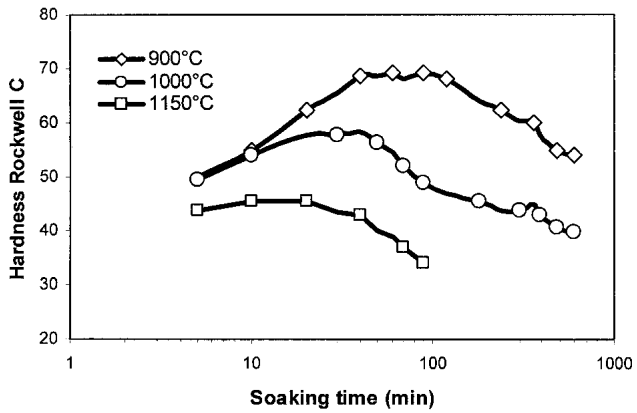

Fig. 18 Bulk hardness of the alloy as a function of the soaking time during the destabilization heat treatment

- Matrix hardness showed a maximum when plotted against soaking time due to these precipitation processes and to the transformation of austenite to martensite. Maximum hardness was obtained for the samples treated for 1-2 h at 900 °C where the structure showed a high volume fraction of martensite and a high amount of fine, well-dispersed secondary carbide particles.

Acknowledgments

The authors are grateful to the University of Michoacan for funding this project.

References

1. C.P. Tabrett, I.R. Sare, and M.R. Gomashchi: "Microstructure-Property Relationships in High-Chromium White Iron Alloys," *Int. Mater. Rev.,* 1996, *41*(2), pp. 59-82.
2. O.N. Dogan, J.A. Hawk, and G. Laird II: "Solidification Structure and Abrasion Resistance of High Chromium White Irons," *Metall. Mater. Trans. A,* 1997, *28*(6), pp. 1315-27.
3. G. Laird II and G.L.F. Powell: "Solidification and Solid-State Transformation Mechanisms in Si Alloyed High-Chromium White Cast Irons," *Metall. Trans. A,* 1993, *24*(2), pp. 981-88.
4. W.W. Cias: "Austenite Transformation Kinetics and Hardenability of Heat Treated 17.5%Cr White Cast Irons," *Trans. AFS,* 1974, *82*, pp. 317-28.
5. G.L.F. Powell and G. Laird II: "Structure, Nucleation, Growth and Morphology of Secondary Carbides in High Chromium and Cr-Ni White Cast Irons," *J. Mater. Sci.,* 1992, *27*, pp. 29-35.
6. F. Maratray and A. Poulalion: "Austenite Retention in High-Chromium White Irons," *Trans. AFS,* 1982, *90*, pp. 795-804.
7. J.T.H. Pearce: "Structure and Wear Performance of Abrasion Resistant Chromium White Cast Irons," *Trans. AFS,* 1984, *92,* pp. 599-621.
8. M. Kuwano, K. Ogi, A. Sawamoto, and K. Matsuda: "Studies on Precipitation Process of Secondary Carbides in High-Chromium Cast Iron," *Trans. AFS,* 1990, *98,* pp. 725-34.
9. G.L.F. Powell and J.V. Bee: "Secondary Carbide Precipitation in an 18 wt%Cr-1 wt%Mo White Iron," *J. Mater. Sci.,* 1996, *31*, pp. 707-11.
10. C. Kim: "X-Ray Method of Measuring Retained Austenite in Heat Treated White Cast Irons," *J. Heat Treating,* 1979, *1*(2), pp. 43-51.
11. A. Bedolla-Jacuinde: "Microstructure of Vanadium-, Niobium- and Titanium-Alloyed High-Chromium White Cast Irons," *Int. J. Cast Metals Res.,* 2001, *13*(6), pp. 343-61.

12. G. Laird II: "Microstructures of Ni-Hard I, Ni-Hard IV and High-Cr White Cast Irons," *Trans. AFS,* 1991, *99,* pp. 339-57.
13. P. Duppin, J. Saverna, and J.M. Schissler: "A Structural Study of Chromium White Cast Iron," *Trans. AFS,* 1982, *90*, pp. 711-18.
14. F. Maratray: "Choice of Appropriate Compositions for Chromium-Molybdenum White Irons," *Trans. AFS,* 1971, *79,* pp. 121-24.
15. J.D.B. DeMello, M. Duran-Charre, and S. Hamar-Thibualt: "Solidification and Solid State Transformations During Cooling of Chromium-Molybdenum White Cast Irons," *Metall. Trans. A,* 1983, *14*(9), pp. 1793-801.
16. J.W. Choi and S.K. Chang: "Effects of Molybdenum and Copper Additions on Microstructure of High Chromium Cast Iron Rolls," *ISIJ Int.,* 1992, *32*(11), pp. 1170-76.
17. C.R. Loper, Jr. and H.K. Baik: "Influence of Molybdenum and Titanium on the Microstructures of Fe-C-Cr-Nb White Cast Irons," *Trans. AFS,* 1989, *97*, pp. 1001-08.
18. C.P. Tong, T. Suzuki, and T. Umeda: "Eutectic Solidification of High Chromium Cast Irons" in *Proc. IV Int. Symposium on the Physical Metallurgy,* Ed. Materials Research Society, Tokyo, Japan, 1989, pp. 403-10.
19. M. Ikeda, T. Umeda, C.P. Tong, T. Suzuki, N. Niwa, and O. Kato: "Effect of Molybdenum Addition on Solidification Structure, Mechanical Properties and Wear Resistivity of High Chromium Cast Iron," *ISIJ Int.,* 1992, *32*(11), pp. 1157-62.
20. M. Radulovic, M. Fiset, K. Peev, and M. Tomovic: "The Influence of Vanadium on Fracture and Abrasion Resistance in High Chromium White Cast Irons," *J. Mater. Sci.,* 1994, *29,* pp. 5085-94.
21. J.V. Bee, G.L.F. Powell, and B. Bednarz: "A Substructure Within the Austenitic Matrix of High-Chromium White Cast Irons," *Scripta Metall. Mater.,* 1994, *31,* pp. 1735-36.
22. O.N. Dogan and J.A. Hawk: "Effect of Retained Austenite on Abrasion Resistance of High-Cr White Cast Irons," *Trans. AFS,* 1997, *105,* pp. 167-74.
23. D.K. Subramanyam: "Retained Austenite Measurements in High Chromium White Irons," *Trans. AFS,* 1985, *93*, pp. 763-68.